Video Article

# Evaluation of Synaptic Multiplicity Using Whole-cell Patch-clamp Electrophysiology

Julia K. Sunstrum[1], Wataru Inoue[1,2,3]

[1]Neuroscience Program, Schulich School of Medicine and Dentistry, University of Western Ontario

[2]Robarts Research Institute, Schulich School of Medicine and Dentistry, University of Western Ontario

[3]Department of Physiology and Pharmacology, Schulich School of Medicine and Dentistry, University of Western Ontario

Correspondence to: Wataru Inoue at WInoue@robarts.ca

URL: https://www.jove.com/video/59461
DOI: doi:10.3791/59461

Keywords: Neuroscience, Issue 146, Whole-cell patch-clamp electrophysiology, *ex vivo*, synaptic transmission, synaptic gain, multiplicity, paraventricular nucleus of the hypothalamus, corticotropin-releasing hormone, hypothalamus

Date Published: 4/23/2019

Citation: Sunstrum, J.K., Inoue, W. Evaluation of Synaptic Multiplicity Using Whole-cell Patch-clamp Electrophysiology. *J. Vis. Exp.* (146), e59461, doi:10.3791/59461 (2019).

## Abstract

In the central nervous system, a pair of neurons often form multiple synaptic contacts and/or functional neurotransmitter release sites (synaptic multiplicity). Synaptic multiplicity is plastic and changes throughout development and in different physiological conditions, being an important determinant for the efficacy of synaptic transmission. Here, we outline experiments for estimating the degree of multiplicity of synapses terminating onto a given postsynaptic neuron using whole-cell patch clamp electrophysiology in acute brain slices. Specifically, voltage-clamp recording is used to compare the difference between the amplitude of spontaneous excitatory postsynaptic currents (sEPSCs) and miniature excitatory postsynaptic currents (mEPSCs). The theory behind this method is that afferent inputs that exhibit multiplicity will show large, action potential-dependent sEPSCs due to the synchronous release that occurs at each synaptic contact. In contrast, action potential-independent release (which is asynchronous) will generate smaller amplitude mEPSCs. This article outlines a set of experiments and analyses to characterize the existence of synaptic multiplicity and discusses the requirements and limitations of the technique. This technique can be applied to investigate how different behavioral, pharmacological or environmental interventions in vivo affect the organization of synaptic contacts in different brain areas.

## Video Link

The video component of this article can be found at https://www.jove.com/video/59461/

## Introduction

Synaptic transmission is a fundamental mechanism for communication between neurons, and hence, brain function. Synaptic transmission is also labile and can change its efficacy in an activity-dependent manner as well as in response to modulatory signals[1]. Thus, examining synaptic function has been a key focus of neuroscience research. Whole-cell patch clamp electrophysiology is a versatile technique that enables us to understand, by devising experimental designs and data analyses, in-depth biophysical and molecular mechanisms of synaptic transmission. A commonly used approach, perhaps owing to the simplicity of the technique and concept, is the measurement of miniature excitatory/inhibitory postsynaptic currents (mE/IPSCs) under the voltage clamp configuration[2,3,4,5,6]. Individual mPSCs represent the flow of ions through postsynaptic ionotropic receptors (e.g. AMPA and $GABA_A$ receptors) in response to the binding of their respective neurotransmitters released from the presynaptic terminal [7]. Because the recording is obtained in the presence of the voltage-gated $Na^+$ channel blocker tetrodotoxin (TTX), the release is action potential-independent and normally involves a single synaptic vesicle that contains neurotransmitter. Based on this assumption, the average amplitude of mPSCs is widely used as a crude estimate for the quantal size, which represents the number and functionality of postsynaptic receptors opposing a single release site. On the other hand, the frequency of mPSCs is considered to represent a combination of the total number of synapses terminating onto the postsynaptic cell and their average release probability. However, these parameters do not measure another variable-multiplicativity of synapses, or synaptic multiplicity — which is important for the efficacy of synaptic transmission.

Based on the quantal theory of synaptic transmission[7,8,9], the strength of a given connection between a pair of neurons is dependent on three factors: the number of functional synapses (*N*), the postsynaptic response to the release of a single synaptic vesicle (quantal size; *Q*) and the probability of neurotransmitter release ($P_r$). Synaptic multiplicity is equivalent to *N*. The development of synaptic multiplicity or the pruning of multiplicative synapses is plastic throughout development and in different disease states[3,4,6,10]. For this reason, characterizing synaptic multiplicity has important implications for understanding the efficacy of synaptic transmission in health and disease. Techniques, such as electron microscopy can identify structural evidence of synaptic multiplicity by detecting multiple synaptic contacts originating from the same axon onto the same postsynaptic neuron[11,12,13,14]. However, these structurally identified multisynapses can be functionally silent[15,16]. Precise functional examination of *N* requires technically challenging electrophysiological approaches, such as paired whole-cell recordings that can identify whether a given connection has multiple functional release sites and minimal stimulation approaches that aim to recruit a single putative axon.

In this protocol, we describe a simple method for estimating synaptic multiplicity by adopting a method originally developed by Hsia et al[2]. This technique involves the measurement of spontaneous PSCs (sPSCs) and mPSCs using whole-cell patch clamp electrophysiology, which allows us to estimate the degree of synaptic multiplicity across all inputs to a given neuron. As previously defined, synaptic multiplicity reflects the number of synapses between a given pre- and postsynaptic neuron. If multiple synapses are recruited in synchrony by an action potential, there will be a high probability of temporal summation of individual (i.e. quantal) PSCs, generating a greater amplitude PSC. In mPSC recordings (in which action potentials are blocked by TTX), the probability of temporal summation of individual (non-synchronous) mPSCs is low. Using this rationale, synaptic multiplicity can be estimated by comparing the sPSC amplitude (with action potential-dependent release) to the mPSC amplitude.

To examine the existence of multiplicity we describe four experiments and their analyses using glutamatergic EPSCs as an example. However, the same approach can be used for the fast GABAergic/glycinergic transmission (IPSCs). A brief rationale for each experiment is described below. First, as explained above, synaptic multiplicity can be estimated by comparing the amplitude of sEPSCs to mEPSCs. There are two requirements for this approach; 1) presynaptic axons must fire a sufficient number of action potentials during recording, and 2) $P_r$ must be high so that multiple synapses release neurotransmitter upon the arrival of an action potential. In order to meet these requirements, sEPSCs are first recorded in low $Ca^{2+}$ artificial cerebrospinal fluid (aCSF), and then recorded in the presence of a low concentration of the $K^+$ channel antagonist, 4-Aminopyridine (4-AP) to increase action potential firing and $P_r$. Then action potential firing is blocked by TTX and Pr decreased by a voltage-gated $Ca^{2+}$ channel blocker $Cd^{2+}$. The amplitude of sEPSCs (with 4AP) is compared to that of mEPSC (with 4AP, TTX, and $Cd^{2+}$). In the second experiment, $Ca^{2+}$ is replaced by equimolar $Sr^{2+}$ in the aCSF to desynchronize vesicle release. As $Ca^{2+}$ is required for the synchronous release of vesicles, replacement with $Sr^{2+}$ should eliminate the large amplitude sEPSCs that are indicative of multiplicity. Third, mechanistically, multiplicity can result from either multiple synaptic contacts to the same postsynaptic neuron or multivesicular release (i.e. multiple vesicles released within a single synaptic contact)[17,18]. To differentiate between the two types of multiplicity, the third experiment uses a low affinity, fast dissociating competitive antagonist of AMPA receptors, γ-D-glutamylglycine (γ-DGG)[17,18] to determine whether large sEPSC are the result of the temporal summation of independent synapses or multivesicular release acting on an overlapping population of postsynaptic receptors. If the large amplitude events arise from multivesicular release, γ-DGG will be less effective at inhibiting larger compared to smaller sEPSCs, whereas large sEPSCs that arise from the temporal summation of multiple synaptic contacts will be similarly affected by γ-DGG. In the fourth experiment, a more physiological method is used to enhance action potential firing, namely afferent synaptic stimulation. Bursts of synaptic activity can transiently increase/facilitate the spontaneous action potential firing and release probability of the stimulated afferents. Therefore, this approach allows multiplicity to manifest in a more physiological manner.

The following protocol describes the method for conducting these experiments in mouse hypothalamic tissue. Specifically, corticotropin releasing hormone (CRH) neurons of the paraventricular nucleus of the hypothalamus (PVN) are used. We describe the procedures for conducting whole-cell patch clamp electrophysiology and explain the specific experiments to test for synaptic multiplicity.

## Protocol

All animal experiments are approved by the Animal Care Committee of The University of Western Ontario in accordance with the Canadian Council on Animal Care Guidelines (AUP#2014-031).

# 1. Solutions

1. **Slicing solution**
    1. Refer to **Table 1** for the composition of the slicing solution.
    2. Prepare a 20x stock solution in advance and store it at 4 °C for up to 1 month.
    3. For 1x slicing solution, dissolve $NaHCO_3$, glucose, and sucrose in $ddH_2O$, and add the 20x stock. Ensure the osmolarity is between 315-320 mOsm and store the solution for no more than 1 week at 4 °C.
    4. Fill two beakers with 100 mL of slicing solution and cover them with parafilm. Chill the solution in a freezer until the solution becomes partially frozen (approximately 20 min in -80 °C freezer). Using a gas dispersion tube, bubble both beakers of slicing solution with 95% $O_2$/5% $CO_2$ for 20 min on ice.

| | Solution Concentrations (mM) | | | | |
|---|---|---|---|---|---|
| | Slicing | Normal aCSF | Low $Ca^{2+}$ aCSF | $Sr^{+}$ aCSF | Pipette/Internal |
| NaCl | 87 | 126 | 126 | 126 | - |
| KCl | 2.5 | 2.5 | 2.5 | 2.5 | 8 |
| $CaCl_2$ | 0.5 | 2.5 | 0.5 | - | - |
| $SrCl_2$ | - | - | - | 2.5 | - |
| $MgCl_2$ | 7 | 1.5 | 2.5 | 1.5 | 2 |
| $NaH_2PO_4$ | 1.25 | 1.25 | 1.25 | 1.25 | - |
| $NaHCO_3$ | 25 | 26 | 26 | 26 | - |
| Glucose | 25 | 10 | 10 | 10 | - |
| Sucrose | 75 | - | - | - | - |
| K-gluconate | - | - | - | - | 116 |
| Na-gluconate | - | - | - | - | 12 |
| HEPES | - | - | - | - | 10 |
| K2-EGTA | - | - | - | - | 1 |
| K2ATP | - | - | - | - | 4 |
| $Na_3GTP$ | - | - | - | - | 0.3 |

**Table 1: The composition of various solutions.**

2. **aCSF (for slice recovery and maintenance)**
    1. Refer to **Table 1** for the composition of the aCSF.
    2. Prepare a 20x stock solution in advance and store it at 4 °C for up to 1 month.
    3. For 1x aCSF, dissolve $NaHCO_3$ and glucose in $ddH_2O$ and add the 20x stock. Ensure the osmolarity is between 298-300 mOsm. Use the solution within 1 day.

3. **aCSF (low $Ca^{2+}$ for recording)**
    1. Refer to **Table 1** for the composition of the low $Ca^{2+}$ aCSF.
    2. Prepare a 20x stock solution in advance and store it at 4 °C for up to 1 month.
    3. For 1x low $Ca^{2+}$ aCSF, dissolve $NaHCO_3$ and glucose in ddH2O and add 20x ($CaCl_2$ and $MgCl_2$ free) stock, $CaCl_2$ and $MgCl_2$ to specified concentrations. Ensure the osmolarity is between 298-300. Use the solution within 1 day.

4. **aCSF ($Sr^{2+}$ for recording)**
    1. Refer to **Table 1** for the composition of the $Sr^{2+}$ aCSF.
    2. Prepare a 20x stock solution in advance and store it at 4 °C for up to 1 month.
    3. For 1x $Sr^{2+}$ aCSF, dissolve $NaHCO_3$ and glucose in $ddH_2O$ and add 20x ($CaCl_2$ and $MgCl_2$ free) stock, $SrCl_2$ and $MgCl_2$ to specified concentrations. Ensure the osmolarity is between 298-300. Use the solution within 1 day.

5. **Internal solution**
    1. Refer to **Table 1** for the composition of the K-gluconate based internal solution.
    2. To make 20 mL of internal solution, add 15 mL of molecular biology grade water to a 50 mL tube. Perform the subsequent steps on the ice.
    3. Prepare the following solutions ahead of time to 1 M stock concentrations in molecular biology grade water. Add (in mL): 2.32 K-gluconate, 0.24 Na-gluconate, 0.20 HEPES, 0.16 KCl, 0.05 K2-EGTA, 0.04 $MgCl_2$ to the 50 mL tube.
    4. Add 100 µL of 0.3 M $Na_3GTP$.
    5. Weigh 44.08 mg of $K_2ATP$ in a 2 mL microcentrifuge tube and add 1 mL of molecular biology grade water, then add to 50 mL tube.
    6. Adjust the pH to 7.2-7.4 with 1 M KOH. Ensure the osmolarity is between 283-289 mOsm.

## 2. Slice Preparation

1. **Prepare tools**
    1. Add 200 mL of aCSF to the recovery chamber (constructed from a 250 mL beaker with 4 wells and netting) and place the recovery chamber in a water bath (35 °C).
    2. Cover the chamber with a paraffin film and constantly bubble the aCSF with 95% $O_2$/5% $CO_2$ using a glass dispersion tube for at least 20 min.
    3. Prepare for the dissection by setting up the tools (scalpel, angled fine scissors, forceps, fine paint brush, plastic spoon).
    4. Fill a 60 mL syringe with approximately 15 mL of the ice-cold slicing solution from step 1.1.4.
    5. Prepare the dissection platform by placing a filter paper on the lid of a well plate.
    6. Prepare the slicing chamber by placing it in the ice tray and filling the tray with ice.

7. Set up the vibratome by securing a disposable blade in the blade holder.
8. Make a transfer pipette by breaking the tip of a Pasteur pipette and placing a rubber bulb over the broken end.

2. **Dissect mouse brain**
    1. Anesthetize the animal in a chamber saturated with 4% isoflurane until spinal reflexes are absent.
    2. Decapitate the animal using a guillotine and quickly remove the brain.
        1. Make a midline incision with a No. 22 scalpel blade from rostral to caudal.
        2. Laterally peel the scalp on each side of the head.
        3. Use fine scissors to cut the skull on one side from caudal to rostral (including the side of the frontal bones), using caution not to damage the brain.
        4. Use forceps to lift the skull piece off the brain and quickly cool the brain with 15 mL of ice-cold slicing solution using the syringe from step 2.1.4.
        5. Lift the brain out of the skull.
        6. Place the brain in one of the beakers filled with ice-cold slicing solution (from step 1.1.4) bubbled with 95% $O_2$/5% $CO_2$.

3. **Prepare slices of mouse hypothalamus**
    1. Block the brain for the desired brain area and cut angle (e.g., for coronal hypothalamic slices, trim off the tissue rostral to the optic chiasm and caudal to the pons using a blade and ensure the caudal block has a flat surface perpendicular to the base of the brain).
    2. Using a cut piece of filter paper, pick up the brain from the anterior side and glue the posterior side to the holding plate using instant glue.
    3. Quickly place the holding plate into the slicing chamber and fill the chamber with slicing solution from the second beaker in step 1.1.4.
    4. Secure the slicing chamber and ice tray on the vibratome.
    5. Define the slicing area (anterior and posterior to the brain) and begin slicing 250 µm thickness coronal slices. Recommended parameters: speed 0.10 mm/s, amplitude 2 mm.
    6. Trim the slices to the appropriate size for the desired brain area.
    7. Recover the slices at 35 °C for 30-45 min. Then, remove the recovery chamber from the warming bath and allow the slices to recover at room temperature for an additional 30 min. Keep slices at room temperature for the rest of the day and continue to bubble the bath constantly with 95% $O_2$/5% $CO_2$.

## 3. Whole-cell Patch ClampRecording

1. **Pull the patch pipettes**
    1. Using the suggested parameters for the whole-cell recording from the pipette puller's manual, pull patch pipettes from thick walled glass to a pipette resistance of 3-5 MΩ.
    2. Using a microsyringe (commercial or homemade), fill a pipette tip with filtered internal solution. To make a microsyringe, burn the tip of a 1 mL syringe and allow the tip to fall creating a long fine tip.

2. **Obtain the whole-cell configuration**
    1. Place the recording pipette just above the slice and offset pipette current in the voltage clamp mode. Apply slight positive pressure to the pipette and lock the stopcock.
    2. Select a healthy cell with an intact membrane and approach the cell with the pipette. The positive pressure should cause a slight disturbance in the tissue (i.e. a slow wave in the tissue when entering).
    3. Slowly continue to bring the pipette closer to the cell using a diagonal motion until the pipette forms a small dimple on the cell surface.
    4. Release the positive pressure lock. The cell will begin to form a seal and the resistance will increase above 1 GΩ. In voltage clamp, hold the cell at -68 mV.
    5. Slightly pull away from the cell diagonally to remove excess pressure from the cell.
    6. Compensate for the fast and slow pipette capacitance.
    7. Apply a brief suction through the tube connected to the pipette holder to break through the cell and obtain whole-cell configuration.
    8. Switch to **Cell** mode on the membrane test window in an electrophysiology Data acquisition and analysis software (e.g., Clampex).
    9. Before each voltage clamp recording, perform a membrane test using the same software and record the relevant parameters in a lab book (membrane resistance, access resistance, and capacitance).
    10. Maintain the temperature of the recording bath at 27–30 °C and the flow rate at 1.5–2.0 mL/min for subsequent experiments.

## 4. Multiplicity Experiments

1. **Experiment 1: estimating multiplicity using 4-AP**
    1. In voltage clamp, hold the cell at -68 mV. Using the same software, record the sEPSCs while perfusing the bath with low $Ca^{2+}$ aCSF. Record for at least 5 min after the start of whole-cell configuration to ensure a stable baseline recording as the synaptic activity may be high shortly after the breakthrough of the membrane.
    2. Using a micropipette, add 4-AP to the aCSF and bath apply 30 µM 4-AP. Record sEPSCs for at least 10 min to obtain the full drug effect.
    3. Add 0.5 µM TTX and 10 µM $Cd^{2+}$ to the aCSF with 4-AP and record the mEPSCs for at least 10 min.
    4. For offline analysis, use the last 1 min of baseline immediately before the application of 4-AP (in low $Ca^{2+}$ aCSF), the 10th min of 4-AP application and the 10th min of TTX application.

2. **Experiment 2: desynchronize vesicle release using $Sr^{2+}$**
    1. While perfusing the bath with normal $Ca^{2+}$ aCSF (the same as the bath aCSF) record sEPSCs for at least 5 min.

2. Switch from the normal $Ca^{2+}$ aCSF and begin perfusing $Sr^{2+}$ aCSF (from step 1.4) and record sEPSCs.
3. For offline analysis, to determine whether the large amplitude sEPSCs are due to the synchronous release of vesicles, compare the last 1 min of baseline (in normal aCSF) to the $10^{th}$ minute of $Sr^{2+}$ aCSF application.

3. **Experiment 3: test for multivesicular release using γ-DGG**
   1. In low $Ca^{2+}$ aCSF record sEPSCs for at least 5 min.
   2. Add 30 µM 4-AP to the aCSF through the perfusion system. Record sEPSCs for at least 10 min.
   3. Add 200 µM γ-DGG to the aCSF with 4-AP and record the sEPSCs for at least 10 min.
   4. As a control experiment in a separate cell, perform steps 1-3 but apply a low concentration (125 nM) of DNQX instead of γ-DGG.
   5. For offline analysis, analyze the last min of each drug application.

4. **Experiment 4: Stimulate afferent inputs to increase action potential firing.**
   1. Record sEPSCs in normal $Ca^{2+}$ aCSF.
   2. Stimulate the afferents using a monopolar glass electrode filled with aCSF at a rate of 20 Hz for 2 s and repeat 10 times with an inter-burst interval of 20 sec.
   3. For analysis, use the 5,000 ms before the first stimulus as the baseline and compare to the 10-300 ms after the final stimulus and then take the average amplitude and frequency change over 10 trials.

## 5. Analysis

1. Analyze sEPSCs and mEPSCs using a program that detects and analyzes synaptic currents (e.g., Mini Analysis software).
   1. Using this software, use the suggested detection parameters for detecting AMPA Receptor EPSCs (or GABA Receptor EPSCs if recording inhibitory currents).
   2. Use the **Nonstop Analysis function** to detect EPSCs in the recording.
   3. Manually scan each recording to ensure the program is accurately detecting each event (e.g., ensure events are not being missed or counted twice).
   4. Export the event data by copying it to the clipboard and paste it into a data management software (e.g., Excel)
   5. Calculate the average frequency and/or amplitude for each drug treatment and perform the relevant statistical analyses.

## Representative Results

The above protocol describes a method for using whole-cell patch clamp electrophysiology to examine the degree of synaptic multiplicity, using mouse hypothalamic neurons as an example. This slice preparation technique should yield healthy viable cells that do not have a swollen membrane or nucleus (**Figure 1**). Each step in the protocol is important for the health of the tissue and quality of the recordings.

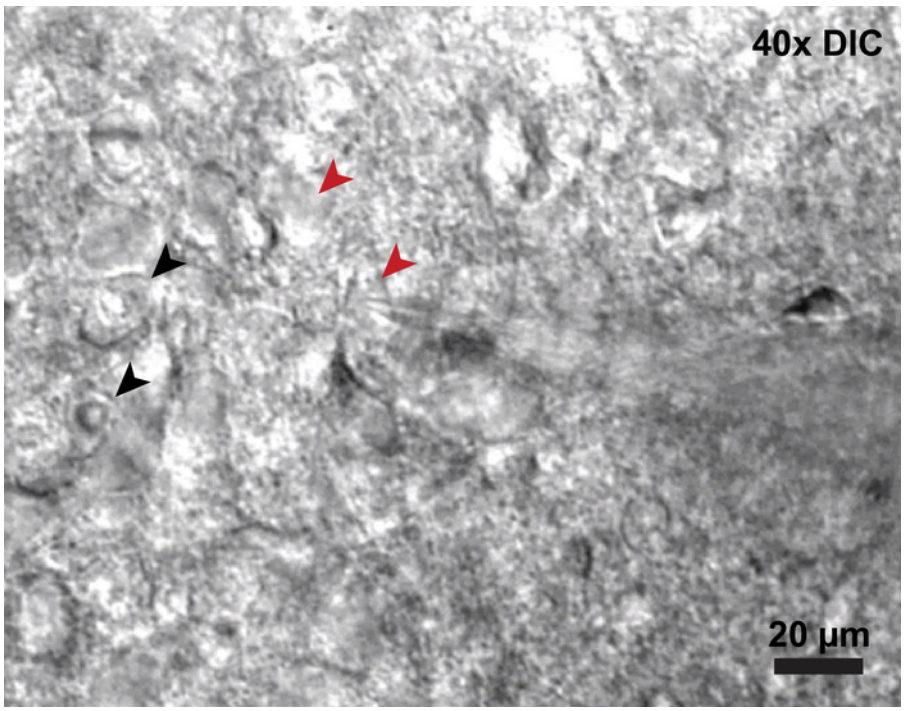


**Figure 1: Healthy and unhealthy tissue following slice preparation.** Slice electrophysiology preparation of the PVN under differential interference contrast optics at 40x magnification. Red arrowheads indicate healthy cells, and black arrowheads indicate unhealthy cells. Please click here to view a larger version of this figure.

**Figure 2** illustrates the rationale for identifying synaptic multiplicity using patch clamp electrophysiology. Synaptic multiplicity can result from either multiple synaptic contact between a pair of neurons (**Figure 2A left**), or by multivesicular release at a given synaptic site (**Figure 2A right**). In both of these situations, an action potential in the presynaptic neuron would elicit a large postsynaptic response (sEPSC) due to the temporal summation of multiple synaptic events. However, in the absence of presynaptic action potentials (e.g. in the presence of TTX and $Cd^{2+}$ to block $Na^{+}$-dependent and $Ca^{2+}$-dependent action potential firing), vesicular neurotransmitter release is asynchronous. As a result, the postsynaptic response becomes smaller (**Figure 2B: AP-independent**). If two neurons do not exhibit multiplicity (i.e. have only one synaptic contact/no multivesicular release) there will be no difference in the postsynaptic response between the action potential-dependent and action potential-independent release of neurotransmitter (**Figure 2C**).

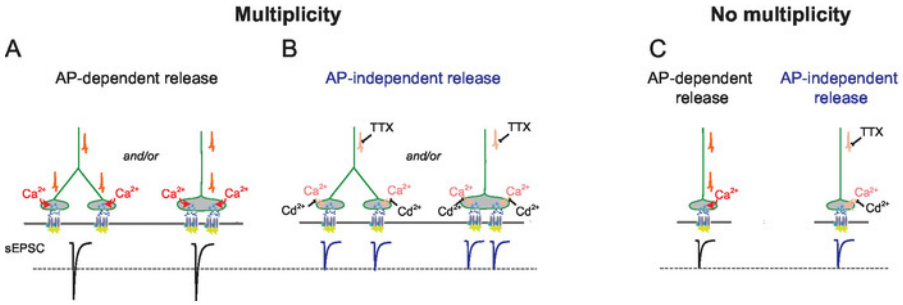


**Figure 2: Schematic diagram illustrating the consequences of different synaptic organizations on postsynaptic currents.** (**A**, **B**) In a synapse with multiplicity, an action potential and the ensuing $Ca^{2+}$ influx triggers synchronous fusion of multiple synaptic vesicles that result in large, multiquantal EPSCs. Synaptic multiplicity can result from multisynapse contact or multivesicular release at a single synapse (A). In the presence of TTX and $Cd^{2+}$, action potential-independent vesicle fusion is asynchronous and causes small uniquantal EPSCs (B). (**C**) In synapses without multiplicity, both action potential-dependent and -independent vesicle fusion results in uniquantal EPSCs. This figure has been modified from **Figure 1A** of our previous report[6]. Please click here to view a larger version of this figure.

In Experiment 1, 4-AP is applied to the bath to increase action potential firing and release probability. To ensure that 4-AP is increasing spontaneous action potential firing, the frequency of EPSCs can be compared between sEPSCs and mEPSCs (**Figure 3A, C**). Because sEPSCs are a combination of both action potential-dependent and -independent events, the difference in the frequency of sEPSC and mEPSC serves as a proxy for spontaneous action potential firing in the presynaptic axons. We use an arbitrary cut off of a > 15% difference in frequency between sEPSC to mEPSC to ensure that a sufficient number of action potential-dependent events are present for the analysis of multiplicity. If the EPSCs in the low $Ca^{2+}$ condition and the TTX (mEPSC) condition are similar in frequency and amplitude (i.e. no spontaneous action potential firing in the low $Ca^{2+}$ condition), the difference between the low $Ca^{2+}$ baseline sEPSC and 4-AP can also be used for the analysis of multiplicity.

In an example result shown in **Figure 3**, 4-AP increases both the amplitude and frequency of sEPSCs. Subsequent application of TTX and $Cd^{2+}$ decreases both the amplitude and frequency. As described above, the difference in the amplitude between sEPSCs and mEPSCs indicates synaptic multiplicity. In the hypothalamic neurons we examine here, the amplitude and frequency of the baseline and TTX conditions are the same (**Figure 3C, D**), suggesting that the baseline sEPSCs contain very few action potential-dependent EPSCs. Accordingly, subsequent experiments can compare the difference between baseline and 4-AP to measure multiplicity.

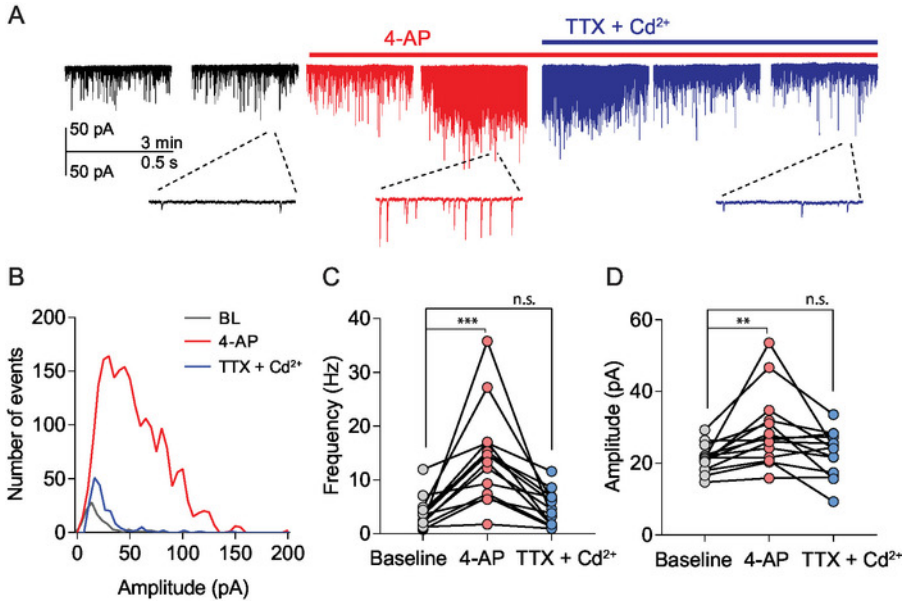


**Figure 3:. 4-AP application reveals synaptic multiplicity.** (**A**) Sample traces of sEPSCs recorded in low $Ca^{2+}$ aCSF during baseline, and after 4-AP (30 µM) application, and subsequent TTX (0.5 µM) and $Cd^{2+}$ (10 µM) application. (**B**) The distribution of sEPSC amplitude from the recording shown in (A). (**C**, **D**) Summary of the mean frequency (C) and amplitude (D) between baseline (grey), 4-AP (red) and TTX +$Cd^{2+}$ (blue). ***P < 0.005, **P < 0.01. This figure has been modified from **Figure 2** of our previous report[6]. Please click here to view a larger version of this figure.

The method described above estimates the average multiplicity of synapses terminating onto the postsynaptic neurons: it may not detect changes in multiplicity that occur to a small proportion of synapses. Nevertheless, in our recent study, this method revealed changes in the multiplicity of glutamate synapses at hypothalamic neurons between normal and chronically stressed conditions[6].

Substitution of $Ca^{2+}$ with equimolar $Sr^{2+}$ in the aCSF desynchronizes action potential-dependent release of neurotransmitter vesicles [19, 20]. Therefore, if the large amplitude sEPSCs are the summation of action potential-dependent synchronized vesicular neurotransmitter release (i.e., multiplicity), replacing $Ca^{2+}$ with $Sr^{2+}$ will decrease the amplitude of EPSCs. As seen in **Figure 4,** $Sr^{2+}$ aCSF decreases the proportion of large amplitude events (**Figure 4B**), and as a consequence decreases the average amplitude (**Figure 4C**). When cells do not exhibit multiplicity, desynchronizing vesicle release will have no effect on the EPSC amplitude.

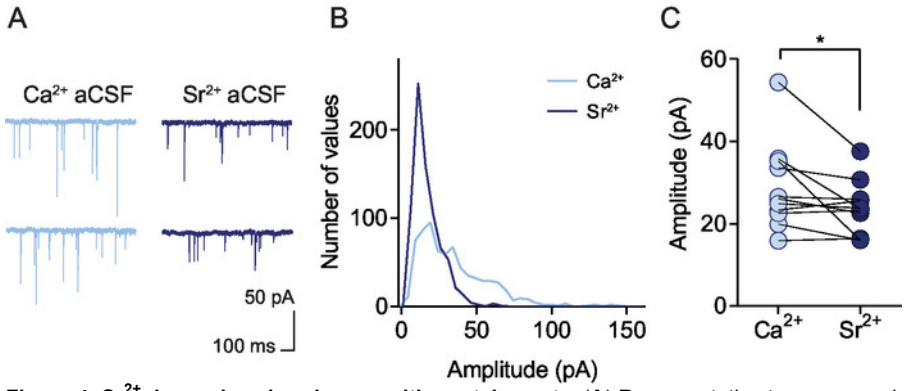


**Figure 4: $Sr^{2+}$ desynchronizes large multiquantal events.** (**A**) Representative trace comparison between normal $Ca^{2+}$ aCSF and $Sr^{2+}$ aCSF. $Sr^{2+}$ aCSF desynchronizes vesicle release and decreases the amplitude of multiquantal synchronous events as seen in a representative amplitude distribution (**B**) and the amplitude change for all cells (**C**) *P < 0.05. This figure has been modified from **Figure 3** of our previous report[6]. Please click here to view a larger version of this figure.

γ-DGG, a fast dissociating competitive antagonist of AMPA receptors, can be used to determine whether multiplicity is due to the multivesicular release or multiple synaptic contacts. As multivesicular release acts on an overlapping population of postsynaptic receptors, the large amplitude EPSCs involves the pooling of glutamate in the synaptic cleft. In other words, the concentration of glutamate in the synaptic cleft is higher than that which results from uniquantal release. On the other hand, multisynaptic contacts would have uniquantal EPSCs at each synaptic site. If the large amplitude EPSCs arise from multivesicular release, the larger EPSCs will be less impacted by γ-DGG antagonism (due to higher glutamate concentration) compared to smaller amplitude EPSCs (**Figure 5A Right, B-D**). If the large amplitude EPSCs are due to the summation of synchronous uniquantal EPSCs (multisynapse contacts), γ-DGG will similarly impact the amplitude of all EPSCs (**Figure 5A Left, E-G**). In contrast to γ-DGG, DNQX which is a high affinity, slow dissociating AMPA/kainate receptor antagonist causes a uniform decrease across all large and small amplitude EPSCs **(Figure 5H-J)**. The sensitivity to γ-DGG and DNQX can be quantified as the ratio of the average EPSC amplitude divided by the maximum (the average of the largest 20 EPSCs) EPSC amplitude **(Figure 5K, L)**.

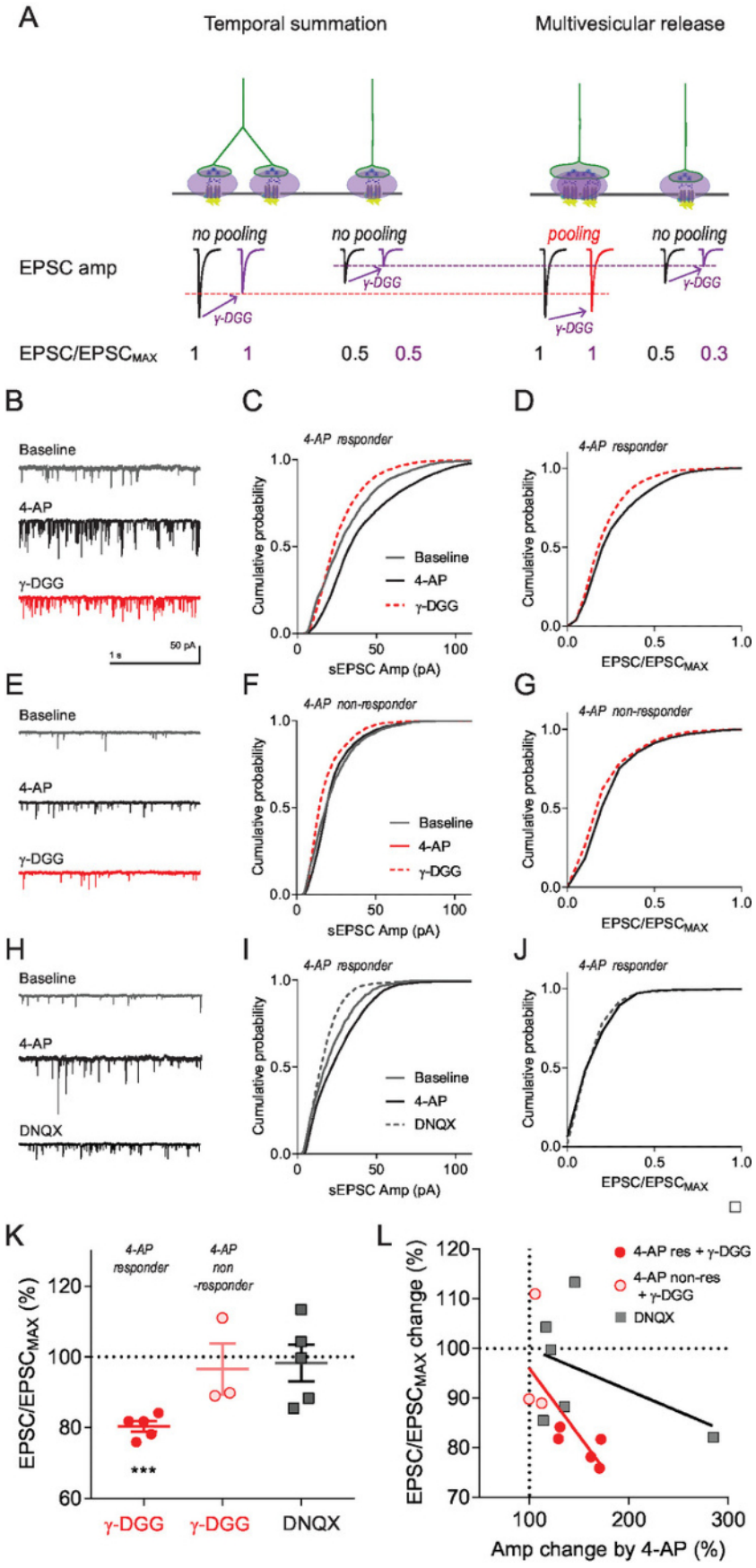
A
Temporal summation
Multivesicular release
no pooling
no pooling
pooling
no pooling
EPSC amp
γ-DGG
γ-DGG
γ-DGG
γ-DGG
EPSC/EPSCMAX 1 1 0.5 0.5 1 1 0.5 0.3
B
Baseline
4-AP
γ-DGG
50 pA
1 s
C
4-AP responder
Cumulative probability
Baseline
4-AP
γ-DGG
sEPSC Amp (pA)
D
4-AP responder
Cumulative probability
EPSC/EPSCMAX
E
Baseline
4-AP
γ-DGG
F
4-AP non-responder
Cumulative probability
Baseline
4-AP
γ-DGG
sEPSC Amp (pA)
G
4-AP non-responder
Cumulative probability
EPSC/EPSCMAX
H
Baseline
4-AP
DNQX
I
4-AP responder
Cumulative probability
Baseline
4-AP
DNQX
sEPSC Amp (pA)
J
4-AP responder
Cumulative probability
EPSC/EPSCMAX
K
4-AP responder
4-AP non-responder
EPSC/EPSCMAX (%)
***
γ-DGG
γ-DGG
DNQX
L
4-AP res + γ-DGG
4-AP non-res + γ-DGG
DNQX
EPSC/EPSCMAX change (%)
Amp change by 4-AP (%)

**Figure 5: Using γ-DGG to probe multivesicular release.** (**A**) Schematics illustrating two models of multiplicity. Left: temporal summation of uniquantal transmission that targets independent populations of postsynaptic receptors. Large and small EPSCs are achieved by a similar glutamate concentration in the synaptic cleft and therefore are equally sensitive to γ-DGG. Right: multiquantal transmission that targets an overlapping population of postsynaptic receptors. Large EPSCs are caused by higher glutamate concentration in the cleft than smaller sEPSCs and are therefore less sensitive to γ-DGG. Values shown at bottom of model are hypothetical relative amplitudes. (**B**) Sample traces from a recording in which there was an increase in mean sEPSC amplitude following 4-AP application (4-AP responder). (**C**) cumulative plot for EPSC amplitude for the recording shown in (B). (**D**) Cumulative plot for normalized EPSC amplitude ($EPSC/EPSC_{MAX}$) before and after application of γ-DGG from the recording shown in (B). (**E**) Sample traces from a recording where there was no change in the mean sEPSC amplitude following 4-AP application (4-AP non-responder). (**F**) Cumulative EPSC amplitude for the recording shown in (E). (**G**) Cumulative $EPSC/EPSC_{MAX}$ plot for the recording shown in (E). (**H**) Sample traces from a recording from baseline, as well as after 4-AP and DNQX application. (**I**) The cumulative EPSC amplitude for the recording shown in (H). (**J**) Cumulative $EPSC/EPSC_{MAX}$ plot for the recording shown in (H). (**K**) Summary of mean $EPSC/EPSC_{MAX}$ after γ-DGG (in 4-AP responder and non-responder groups) or DNQX application normalized to pre-γ-DGG/DNQX (i.e. post-4-AP). (**L**) Plots of post-4-AP mean EPSC amplitude (normalized to pre-4-AP) against post-γ-DGG/DNQX mean $EPSC/EPSC_{MAX}$ (normalized to post-4-AP). ***P < 0.005. This figure has been modified from **Figure 4** of our previous report[6]. Please click here to view a larger version of this figure.

The strength of synaptic transmission can be transiently increased by bursts of synaptic activity. To investigate multiplicity under more physiological conditions, afferent stimulation can be used to increase action potential firing and release probability. If multiplicity is present, afferent stimulation should cause a brief increase in the EPSC amplitude (**Figure 6A-D**). If multiplicity is not present, activity driven increases in action potential firing will not increase the EPSC amplitude.

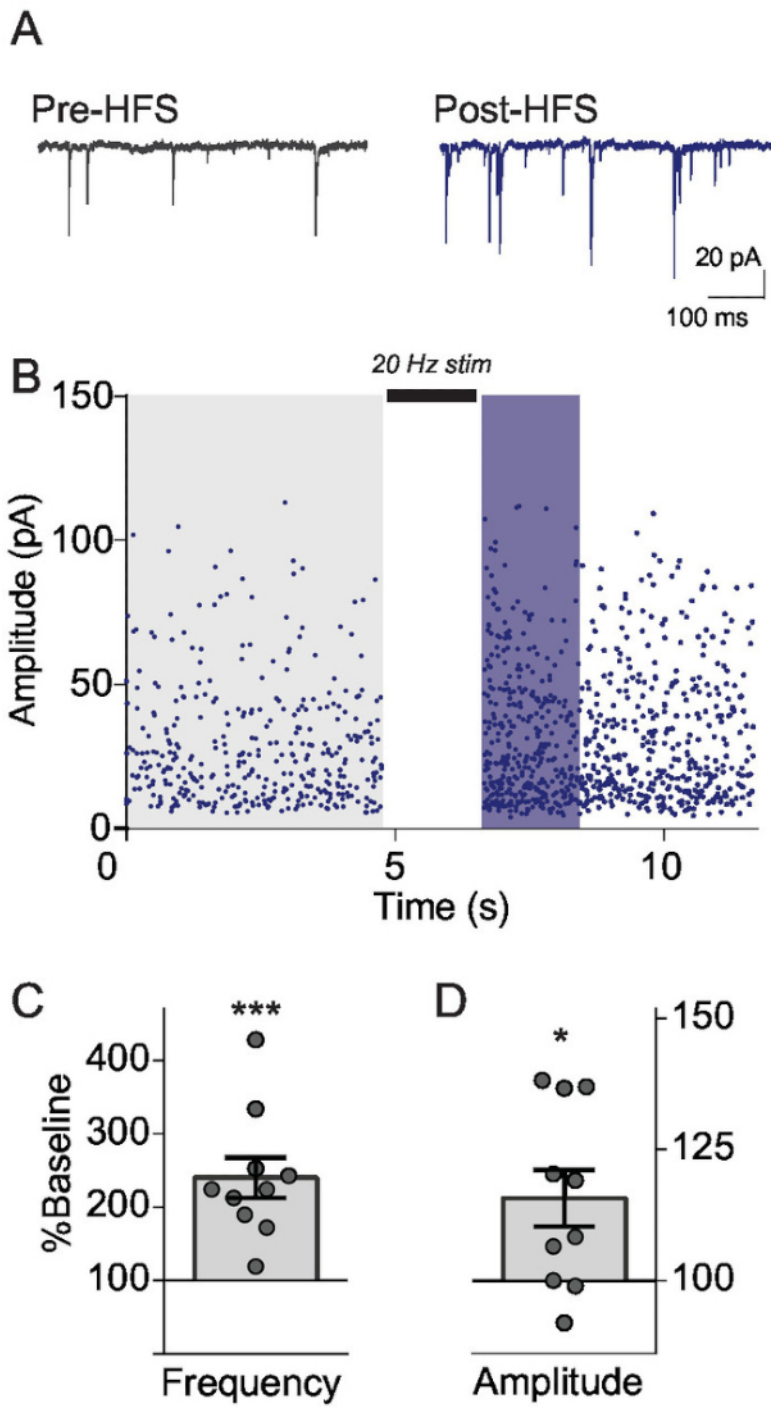


**Figure 6: High-frequency stimulation reveals synaptic multiplicity.** (**A**) Sample traces of sEPSCs before and after afferent synaptic stimulation. (**B**) plot of sEPSC amplitude before and after synaptic stimulation (20 Hz, 2 s) from the recording shown in (A). (**C**, **D**) Summary of sEPSC frequency (C) and amplitude (D) changes following synaptic stimulation. ***P < 0.001, *P < 0.05. This figure has been modified from **Figure 5** of our previous report[6]. Please click here to view a larger version of this figure.

## Discussion

One important requirement for a successful patch clamp electrophysiology experiment is obtaining healthy slices/cells. Our described protocol is optimized for hypothalamic slices that contain PVN neurons. Other brain areas may require modified solutions and slicing methods[21,22,23,24]. For the recording, it is critical to only accept stable recordings by constantly monitoring cell properties such as membrane resistance, capacitance and access resistance. An increase in access resistance can decrease EPSC amplitude and therefore confound amplitude measurements. Accordingly, cells with access resistance values that exceed 20 MΩ or increase by more than 20% during recording are discarded. Similarly, a decrease in (or a low) membrane resistance can result in poor space-clamp and, therefore, can decrease the amplitude. The neurons in our

target system (parvocellular PVN neurons) have a high membrane resistance between 500 MΩ and 1 GΩ, and we discard cells with membrane resistances below 500 MΩ. Quality control cut-offs should be established for specific types of neurons under study. As this protocol relies on the difference in the amplitude before and after drug applications, it is important to ensure that the amplitude change is due to the drug application and not to the changes in membrane resistance and access resistance. The hypothalamic neurons we study in this protocol are small in size (cell capacitance is about 15 pF in mice and membrane resistance is around 1 GΩ), and K-gluconate based internal solution works well to obtain high quality EPSCs/IPSCs[6,25]. For neurons with larger cell size and low input resistance, cesium based internal solution can be used to ensure a good space-clamp[2].

One specific requirement of using this method to measure the multiplicity is that the cells fire a sufficient number of spontaneous action potentials in order to compare action potential-dependent events to mEPSCs. This can be ensured by comparing the difference in the frequency of EPSCs in the absence and presence of TTX and $Cd^{2+}$. In hypothalamic slices that contain the PVN, we have found that the application of 4-AP is efficient to elicit action potential firing. Another method, pioneered by Hsia and colleagues[2], uses high $Ca^{2+}$ aCSF to increase action potential firing, rather than 4-AP. While this method was successful in hippocampal slices, we found that the high $Ca^{2}$+ was less efficient than 4-AP in facilitating action potential firing in hypothalamic slices[6]. Indeed, it has been shown that high, extracellular $Ca^{2+}$ concentration decreases intrinsic excitability of neurons and axons by altering $Na^{+}$ conductance[26, 27]. This may explain why in some slices, high $Ca^{2+}$ aCSF is not effective in increasing EPSC frequency.

One limitation of this method, which is inherent to all slice patch clamp electrophysiology, is that many, long-range projections to the postsynaptic neurons are cut in slice preparations. In order to observe action potentials, it is likely that the presynaptic axons and cell bodies need to be preserved in the slice. Therefore, the multiplicity measurement is skewed to synaptic connectivity that is preserved within the slice. Along the same line, the direction of slicing may cause certain populations of projections to be preserved while others are severed[28]. These limitations have a general effect of underestimating the multiplicity of afferent inputs.

The described protocol provides a method for estimating the degree of synaptic multiplicity across all inputs to a given neuron. Other electrophysiology techniques, such as paired recordings or minimal stimulation of a single axon can identify whether a given connection has multiple contacts, but these experiments are often difficult and not possible in all systems. Further, they cannot give an overall indication of the organization of all of the inputs to a given neuron as they only isolate one pair of neurons. The present protocol uses basic patch-clamp electrophysiology methods to evaluate the degree of multiplicity across all inputs to a given neuron.

## Disclosures

The authors have nothing to disclose

## Acknowledgments

J.S. received Ontario Graduate Scholarship. W.I. received a New Investigator Fellowship from Mental Health Research Canada. This work is supported by operating grants to W.I from the Natural Sciences and Engineering Research Council of Canada (06106-2015 RGPIN) and the Canadian Institute for Health Research (PJT 148707).

## References

1. Abbott, L.F., Nelson, S.B. Synaptic plasticity: taming the beast. *Nature Neuroscience.* **3** (Supp), 1178–1183 (2000).
2. Hsia, A.Y., Malenka, R.C., Nicoll, R.A. Development of Excitatory Circuitry in the Hippocampus. *Journal of Neurophysiology.* **79** (4), 2013–2024 (1998).
3. Zhan, Y. *et al.* Deficient neuron-microglia signaling results in impaired functional brain connectivity and social behavior. *Nature neuroscience.* **17** (3), 400–6 (2014).
4. Paolicelli, R.C. *et al.* Synaptic pruning by microglia is necessary for normal brain development. *Science (New York, N.Y.).* **333** (6048), 1456–8 (2011).
5. Schrader, L.A., Tasker, J.G. Presynaptic Modulation by Metabotropic Glutamate Receptors of Excitatory and Inhibitory Synaptic Inputs to Hypothalamic Magnocellular Neurons. *Journal of Neurophysiology.* **77** (2), 527–527 (1997).
6. Salter, E.W., Sunstrum, J.K., Matovic, S., Inoue, W. Chronic stress dampens excitatory synaptic gain in the paraventricular nucleus of the hypothalamus. *The Journal of Physiology.* **596** (17), 4157–4172 (2018).
7. Redman, S. Quantal analysis of synaptic potentials in neurons of the central nervous system. *Physiological Reviews.* **70** (1), 165–198 (1990).
8. Del Castillo, J., Katz, B. Quantal components of the end-plate potential. *The Journal of physiology.* **124** (3), 560–73, at <http://www.ncbi.nlm.nih.gov/pubmed/13175199> (1954).
9. Stevens, C.F. Quantal release of neurotransmitter and long-term potentiation. *Cell.* **72 Suppl**, 55–63, at <http://www.ncbi.nlm.nih.gov/pubmed/8094037> (1993).
10. Deger, M., Helias, M., Rotter, S., Diesmann, M. Spike-timing dependence of structural plasticity explains cooperative synapse formation in the neocortex. *PLoS computational biology.* **8** (9), e1002689 (2012).
11. van den Pol, A.N., Wuarin, J.P., Dudek, F.E. Glutamate, the dominant excitatory transmitter in neuroendocrine regulation. *Science (New York, N.Y.).* **250** (4985), 1276–1278, at <http://www.ncbi.nlm.nih.gov/pubmed/1978759> (1990).
12. Miklós, I.H., Kovács, K.J. Reorganization of synaptic inputs to the hypothalamic paraventricular nucleus during chronic psychogenic stress in rats. *Biological Psychiatry.* **71** (4), 301–308 (2012).
13. Korn, H., Triller, A., Mallet, A., Faber, D.S. Fluctuating responses at a central synapse: n of binomial fit predicts number of stained presynaptic boutons. *Science (New York, N.Y.).* **213** (4510), 898–901, at <http://www.ncbi.nlm.nih.gov/pubmed/6266015> (1981).
14. Tracey, D.J., Walmsley, B. Synaptic input from identified muscle afferents to neurones of the dorsal spinocerebellar tract in the cat. *The Journal of physiology.* **350**, 599–614, at <http://www.ncbi.nlm.nih.gov/pubmed/6747859> (1984).

 

15. Lin, J.W., Faber, D.S. Synaptic transmission mediated by single club endings on the goldfish Mauthner cell. II. Plasticity of excitatory postsynaptic potentials. *The Journal of neuroscience : the official journal of the Society for Neuroscience.* **8** (4), 1313–25, at <http://www.ncbi.nlm.nih.gov/pubmed/2833581> (1988).
16. Atwood, H.L., Tse, F.W. Changes in binomial parameters of quantal release at crustacean motor axon terminals during presynaptic inhibition. *The Journal of physiology.* **402**, 177–93, at <http://www.ncbi.nlm.nih.gov/pubmed/2907048> (1988).
17. Li, G.-L., Keen, E., Andor-Ardó, D., Hudspeth, A.J., von Gersdorff, H. The unitary event underlying multiquantal EPSCs at a hair cell's ribbon synapse. *The Journal of neuroscience : the official journal of the Society for Neuroscience.* **29** (23), 7558–68 (2009).
18. Wadiche, J.I., Jahr, C.E. Multivesicular release at climbing fiber-Purkinje cell synapses. *Neuron.* **32** (2), 301–13, at <http://www.ncbi.nlm.nih.gov/pubmed/11683999> (2001).
19. Oliet, S.H., Malenka, R.C., Nicoll, R.A. Bidirectional control of quantal size by synaptic activity in the hippocampus. *Science (New York, N.Y.).* **271** (5253), 1294–7, at <http://www.ncbi.nlm.nih.gov/pubmed/8638114> (1996).
20. Inoue, W. *et al.* Noradrenaline is a stress-associated metaplastic signal at GABA synapses. *Nature Neuroscience.* **16** (5), 605–612 (2013).
21. Ting, J.T., Daigle, T.L., Chen, Q., Feng, G. Acute Brain Slice Methods for Adult and Aging Animals: Application of Targeted Patch Clamp Analysis and Optogenetics. *Methods in molecular biology (Clifton, N.J.).* **1183**, 221–242 (2014).
22. Richerson, G.B., Messer, C. Effect of composition of experimental solutions on neuronal survival during rat brain slicing. *Experimental neurology.* **131** (1), 133–43, at <http://www.ncbi.nlm.nih.gov/pubmed/7895807> (1995).
23. Tanaka, Y., Tanaka, Y., Furuta, T., Yanagawa, Y., Kaneko, T. The effects of cutting solutions on the viability of GABAergic interneurons in cerebral cortical slices of adult mice. *Journal of neuroscience methods.* **171** (1), 118–25 (2008).
24. Ye, J.H., Zhang, J., Xiao, C., Kong, J.-Q. Patch-clamp studies in the CNS illustrate a simple new method for obtaining viable neurons in rat brain slices: glycerol replacement of NaCl protects CNS neurons. *Journal of neuroscience methods.* **158** (2), 251–9 (2006).
25. Gunn, B.G. *et al.* Dysfunctional astrocytic and synaptic regulation of hypothalamic glutamatergic transmission in a mouse model of early-life adversity: relevance to neurosteroids and programming of the stress response. *Journal of Neuroscience.* **33** (50), 19534–19554 (2013).
26. Su, H., Alroy, G., Kirson, E.D., Yaari, Y. Extracellular calcium modulates persistent sodium current-dependent burst-firing in hippocampal pyramidal neurons. *The Journal of neuroscience : the official journal of the Society for Neuroscience.* **21** (12), 4173–82, at <http://www.ncbi.nlm.nih.gov/pubmed/11404402> (2001).
27. Frankenhaeuser, B., Hodgkin, A.L. The action of calcium on the electrical properties of squid axons. *The Journal of physiology.* **137** (2), 218–44, at <http://www.ncbi.nlm.nih.gov/pubmed/13449874> (1957).
28. Xiong, G., Metheny, H., Johnson, B.N., Cohen, A.S. A Comparison of Different Slicing Planes in Preservation of Major Hippocampal Pathway Fibers in the Mouse. *Frontiers in neuroanatomy.* **11**, 107 (2017).


 